Hindawi
Journal of Electrical and Computer Engineering
Volume 2023, Article ID 9757630, 1 page
https://doi.org/10.1155/2023/9757630

Retraction

Retracted: Smart System Resource Coordination Algorithm Based on 6G Technology

Journal of Electrical and Computer Engineering

Received 19 December 2023; Accepted 19 December 2023; Published 20 December 2023

This article has been retracted by Hindawi following an investigation undertaken by the publisher [1]. This investigation has uncovered evidence of one or more of the following indicators of systematic manipulation of the publication process:

(1) Discrepancies in scope

(2) Discrepancies in the description of the research reported

(3) Discrepancies between the availability of data and the research described

(4) Inappropriate citations

(5) Incoherent, meaningless and/or irrelevant content included in the article

(6) Manipulated or compromised peer review

The presence of these indicators undermines our confidence in the integrity of the article's content and we cannot, therefore, vouch for its reliability. Please note that this notice is intended solely to alert readers that the content of this article is unreliable. We have not investigated whether authors were aware of or involved in the systematic manipulation of the publication process.

Wiley and Hindawi regrets that the usual quality checks did not identify these issues before publication and have since put additional measures in place to safeguard research integrity.

We wish to credit our own Research Integrity and Research Publishing teams and anonymous and named external researchers and research integrity experts for contributing to this investigation.

The corresponding author, as the representative of all authors, has been given the opportunity to register their agreement or disagreement to this retraction. We have kept a record of any response received.

References

[1] F. Wang, "Smart System Resource Coordination Algorithm Based on 6G Technology," *Journal of Electrical and Computer Engineering*, vol. 2022, Article ID 2688385, 12 pages, 2022.

Hindawi
Journal of Electrical and Computer Engineering
Volume 2022, Article ID 2688385, 12 pages
https://doi.org/10.1155/2022/2688385

Research Article

Smart System Resource Coordination Algorithm Based on 6G Technology

Fang Wang

Computer School, Hubei University of Education, Wuhan 430205, China

Correspondence should be addressed to Fang Wang; wangfangbabyfang@163.com

Received 4 March 2022; Revised 8 April 2022; Accepted 18 April 2022; Published 9 May 2022

Academic Editor: Wei Liu

Most of the existing resource allocation algorithms do not take into account the restriction conditions such as the delay limitation of different services and the service volume requirements of different STAs. Moreover, the surge in the number of smart terminal devices has brought great challenges to the access effect of WLAN systems. Therefore, 6G technology will surely replace the current technology as the main means of future communication technology. This paper combines 6G technology to study the smart system resource coordination algorithm and analyzes the calculation process and actual effect of the algorithm. Moreover, this paper analyzes the coordination of smart system resources and verifies the effect of 6G technology in the coordination of smart system resources through experimental research. The results of experimental research show that the smart system resource coordination algorithm based on 6G technology can effectively improve the resource coordination effect of smart systems and has certain anti-interference, which will promote the construction of smart systems in the future.

1. Introduction

In recent years, in addition to being used for mobile access, WLAN has also been used in application scenarios such as small base station data backhaul and camera data backhaul. Traditional WLAN access networks have high requirements for throughput but are not sensitive enough to indicators such as reliability and link delay. Its MAC layer is based on the CSMA/CA competition access mechanism based on the distributed coordination function (DCF) and uses the binary exponential backoff algorithm [1]. Since only one AP or STA can occupy a channel at the same time, as the number of STAs and APs increases, multiple nodes compete for the channel at the same time, and the probability of collisions will increase exponentially, resulting in an exponential decline in node throughput. However, the WLAN network used as the data backhaul function has high requirements on delay, throughput, and packet loss rate, and the existing MAC working mechanism of the WLAN cannot meet the requirements. Therefore, it is necessary to study the MAC access mechanism based on centralized control suitable for the WLAN data backhaul network [2].

In scenarios where AP deployment is relatively intensive, there will be overlapping basic service set (OBSS) areas between adjacent basic service sets (BSSs). If the RUs of users in the OBSS area are non-orthogonal, they may be interfered by neighboring users and affect system performance [3].

The working mechanism of 802.11ax is based on AP scheduling access, supplemented by competitive access. The 802.11ax protocol is compatible with the EDCA mechanism. By setting different queue priorities and channel competition parameters, multiple STAs are allowed to access the channel at the same time through competition or scheduling, providing a certain degree of user quality of service (QoS) for STAs of different service types, which also reduces the probability of collision. When WLAN is used for data backhaul applications, multiple APs are usually deployed next to each other, and there may be overlapping areas between the antenna coverage of adjacent APs, which makes co-channel interference between BSSs more serious. In the existing WLAN standard, each AP node is peer-to-peer, and the AP can only control each STA associated with it, and information interaction or cooperation between APs cannot be carried out. The operation is relatively simple, but the

efficiency and network performance are low. The WLAN anti-interference mechanism based on cooperation among multiple APs or based on the centralized controller AC is a more recognized direction in the industry in the future. By managing resources through global information, better system performance can be obtained.

Most of the existing resource allocation algorithms do not take into account the time delay restrictions of different services and the service volume requirements of different STAs. The number of smart terminal devices has increased sharply, and the access mechanism of WLAN technology has been greatly challenged. At present, all kinds of smart terminal devices have been with us, and new products will be released every year. Cisco forecasted that by 2021, the total number of wirelessly connected devices will exceed 20 billion. As the main carrier of mobile traffic, WLAN will increase its user density rapidly. The MAC layer access of traditional WLAN equipment is based on the carrier-sense multiple access with collision avoidance (CSMA/CA) mechanism of collision avoidance, and users use a competitive method to access the channel. In the case of intensive terminal access, the probability of contention collisions will greatly increase, leading to waste of resources in the competition backoff process most of the time, resulting in a decrease in system throughput. Studies have shown that the MAC efficiency of traditional WLAN systems in dense scenarios is only 33%–40%. In the second aspect, in order to meet the needs of users, the deployment density of wireless network access points (APs) has been greatly increased, and the same/overlapped frequency interference in the system has increased.

Based on the 6G technology, this paper studies the smart system resource coordination algorithm, proposes an improved method, and verifies its effectiveness, so as to provide a theoretical reference for the further popularization and development of the follow-up 6G technology.

2. Related Work

The dense deployment of nodes in the next-generation WLAN can provide users with access services anytime and anywhere to achieve a greater degree of spatial reuse and system capacity improvement [4]. In the wireless backhaul network, there is generally a controller that can reasonably allocate wireless network resources according to the channel state information (CSI) and QoS of different users [5]. Siboni et al. [6] analyzed the reliability of WLAN multi-hop backhaul connections in detail, including the possibility of successfully sending data packets, and used an empirical model to evaluate the feasibility of using a multi-hop linear topology in the backhaul network. The evaluation results show that the cost-effective WLAN technology has great potential as a backhaul network and has good stability. Since wireless backhaul networks have higher requirements for throughput, efficient resource allocation strategies are particularly important. Yang et al. [7] proposed a solution to the scheduling, resource allocation, and flow control problems of half-duplex (HD) backhaul networks. It formulates resource allocation and scheduling problems as optimization problems, and its goal is to maximize the sum of transmission rates. Li et al. [8] studied time-varying channel conditions and the problem of delay-aware high-efficiency transmission in wireless backhaul networks under random traffic load. Through comprehensive consideration of subcarrier allocation, power allocation, and transmission time interval, it is expressed as a random optimization problem to maximize system energy efficiency (EE) and ensure network stability. Ray [9] studied energy-efficient resource allocation in a two-layer massive MIMO heterogeneous network with wireless backhaul. Among them, the macro-base station (MBS) adopts millimeter wave frequency communication, and the small base station (SBS) with OFDMA technology adopts the frequency band of cellular communication.

Considering the need for synchronization and reducing overhead in OFDMA, Mayer and Baeumner [10] proposed a framework for multi-user access based on OFDMA's IEEE802.11ax (OMAX) protocol. The protocol uses full-channel carrier sensing and fast backoff procedures to solve the synchronization problem, while designing an enhanced RTS/CTS mechanism and a new frame structure to reduce overhead. Saez et al. [11] analyzed the theoretical limitation of the system efficiency of the 802.11ax random access protocol and proposed an OFDMA-based hybrid channel access (OHCA) method, which can provide STAs with long-term and short-term fair channel access. In the literature [12], the protocol is formulated for the behavior of multiple users accessing the channel at the same time for data transmission. With the deepening of research, Smys et al. [13] proposed a multiple access protocol with QoS guarantee based on OFDMA. The agreement consists of two main programs. One of them is a redundant access mechanism for video traffic transmission, that is, the video service can send multiple RTS packets to the AP at the same time through multiple sub-channels to improve the probability of successful access of the video service. The second is a priority-based resource allocation algorithm that enables APs to allocate more resources for video services. Performance simulation results show that the protocol has excellent performance in terms of video traffic delay and delay jitter. Aiming at the 802.11axOFDMA uplink random access method, Butun et al. [14] proposed a scheme to dynamically adjust its contention window to increase the next contention window of users who occupy the channel for a long time, which aims to improve the fairness of users' access to the channel. Qiu et al. [15] divided services into four access types based on EDCA priority and set different access parameters for different priority services to ensure QoS. Due to the limitation of wireless spectrum resources and the dense deployment of APs may cause serious interference between BSSs, the wireless resource management algorithm for rationally scheduling users and allocating resources can effectively reduce co-channel interference between BSSs, improve the overall performance of the system, and satisfy demand for transmission of diversified business types [16]. The difference is that the smallest resource particle for resource allocation in a cellular network is a resource block (RB), can effectively improve user experience [17]. The resource allocation granularity in 802.11ax is a resource unit

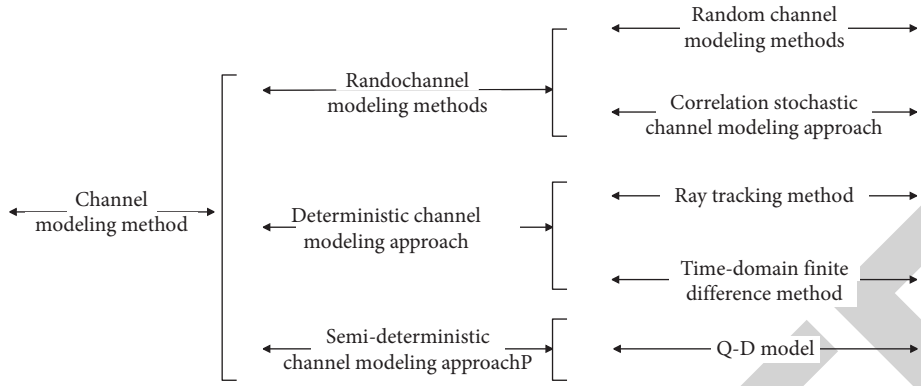

Figure 1: Classification of 6G channel modeling methods.

(RU) that is larger than the RB specification, and the overall network throughput is usually more concerned. A large number of research results show that avoiding the APs of adjacent BSSs to work on the same frequency channel can effectively reduce the co-frequency interference between wireless access points [18]. In a centralized WLAN, the centralized controller AC can centrally allocate the wireless resources of multiple APs and allocate orthogonal channels to different APs as much as possible to avoid co-frequency interference. Although the 2.4 GHz public frequency band for WLAN work is divided into 11 channels with overlapping 22 MHz bandwidth, only three channels 1, 6, and 11 are orthogonal to each other [19], so adjacent APs may not work in orthogonal channels. Since the reasonable allocation of channels helps to reduce the interference in the network and improve the system throughput and spectrum efficiency, non-orthogonal channel allocation has always been a hot issue of research [20].

3. Classification of 6G Channel Modeling Methods

As a component of the communication system, the 6G channel directly affects data transmission. Whether it is the design of the communication system or the continuously expanding communication technology research of new frequency bands, full and thorough 6G channel knowledge is required as a basis. The 6G channel model can well describe the propagation characteristics of the signal in the actual environment and provide references for communication network planning and system design.

There are three 6G channel modeling methods, random 6G channel modeling, deterministic 6G channel modeling, and semi-deterministic 6G channel modeling methods, as shown in Figure 1.

Random 6G channel modeling methods include geometric random 6G channel modeling (GBSM) and correlated random 6G channel modeling (CBSM). Geometric random 6G channel modeling can be further divided into regular shape and irregular shape geometric random 6G channel modeling. Regular shape geometric random 6G channel modeling defines one or more geometric figures, such as spheres, ellipses, cylinders, and so on, according to the communication environment, and distributes different types of scatterers on different regular geometric figures with a certain probability density distribution function. However, the irregular shape geometric random 6G channel modeling assumes that the scatterers are distributed on the irregular shape geometric figure. Through geometric calculation, the 6G channel response of the corresponding path is derived based on parameters such as departure angle, arrival angle, amplitude, phase, and time delay. Finally, the results on the paths corresponding to each scatterer are superimposed to obtain the total 6G channel impulse response, 6G channel transfer function, and so on. The correlation random 6G channel model calculates the parameters of the 6G channel through the correlation between the sub-6G channels and describes the characteristics of the 6G channel.

The deterministic 6G channel modeling method uses geometric optics theory and electromagnetic wave propagation theory. It predicts the 6G channel model based on detailed actual environmental information, including building structure, material properties, and topographic features. Deterministic 6G channel modeling methods include ray tracing method and finite difference time domain method. The ray tracing method is based on geometric optics theory, using rays to simulate the propagation path of a signal, considering the direct, transmission, reflection, and diffraction paths to obtain their signal strength, departure and arrival angle, etc. The finite difference time domain method uses second-order difference equations to solve Maxwell's equations in the time domain. The deterministic 6G channel modeling method has high accuracy, but it is only suitable for static environments. Once the propagation environment changes, the modeling needs to be remodeled, and the complexity will be greatly increased due to the increase of environmental information.

The semi-deterministic 6G channel modeling method includes a quasi-deterministic (Q-D) model, which divides the path into a random path, a deterministic path, and a flash path. It uses the random method to describe the random path and the flash path and the deterministic method to describe the definite path.

At present, there have been a lot of research studies on the measurement and modeling of terahertz 6G channel, but there are few research studies on geometric random terahertz modeling, especially the three-dimensional regular geometric random model. Due to the large attenuation of terahertz

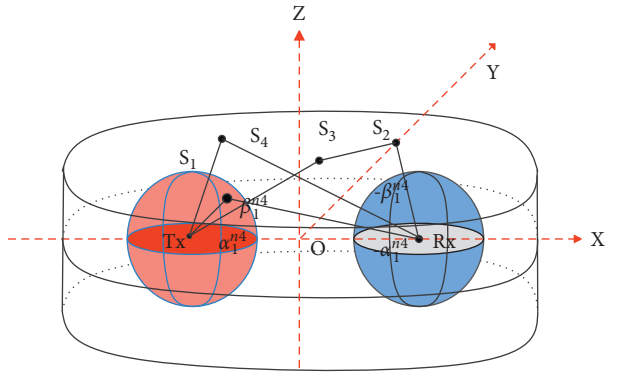

Figure 2: Ellipsoid-double sphere three-dimensional geometric 6G channel model.

communication and because most of the communication scenarios are indoor short-distance communications, the 3D 6G channel model can provide higher accuracy for terahertz 6G channel modeling in small-scale scenarios.

This paper improves the ellipsoid-double sphere model based on the literature. The distribution position of the scatterer adds the top surface of the ellipsoid to model the ceiling, making the model more suitable for indoor communication scenes. The sides of the barrel and the surface of the sphere model the walls and the scatterers around the transmitter and receiver, respectively. Because the ground is often covered by obstacles, its influence is ignored. The sphere centers of the two spheres are located at the two focal points of the ellipsoid, respectively, and the transmitting end Tx and the receiving end Rx are, respectively, placed as shown in Figure 2.

N_l scatterers S_l are distributed on the surface of the sphere at the transmitting end, N_2 scatterers S_2 are distributed on the surface of the sphere at the receiving end, N_3 scatterers S_3 are distributed on the side of the ellipsoid, and N_4 scatterers S_4 are distributed on the top surface of the ellipsoid. Taking the midpoint of the two focal points as the origin and establishing a three-dimensional coordinate system, the transmitter and receiver can be expressed as $Tx(-1D/2, 0, 0)$ and Rx (D/2, 0, 0), respectively, the coordinates of the scatterer S_l can be expressed as $S_l(x_l, y_l, z_l)$. Among them, the coordinate of S_l is

$$\begin{aligned} x_1 &= -\frac{D}{2} + R_t \cos\beta_t^{n_1} \cos\alpha_t^{n_1}, \\ y_1 &= R_t \cos\beta_t^{n_1} \sin\alpha\beta_t^{n_1}, \\ z_1 &= R_t \sin\beta_t^{n_1}. \end{aligned} \tag{1}$$

The coordinates of S_2 can be expressed as

$$\begin{aligned} x_2 &= \frac{D}{2} - R_r \cos\left(-\beta_r^{n_2}\right)\cos\left(-\alpha_r^{n_2}\right), \\ y_2 &= R_r \cos\left(-\beta_r^{n_2}\right)\sin\left(-\alpha_r^{n_2}\right), \\ z_2 &= R_t \sin\left(-\beta_t^{n_2}\right). \end{aligned} \tag{2}$$

Table 1: LoS, SB, and DB components considered by the model.

Component	Path
LoS	Tx-Rx
SB	Tx-S_1-Rx
	Tx-S_2-Rx
	Tx-S_3-Rx
	Tx-S_4-Rx
DB	Tx-S_1-S_2-Rx
	Tx-S_1-S_3-Rx
	Tx-S_1-S_4-Rx
	Tx-S_3-S_2-Rx
	Tx-S_4-S_2-Rx

The coordinates of S_3 can be solved by the following equations:

$$\begin{aligned} y_3 &= \tan\left(\pi + \alpha_r^{n_3}\right)\left(x_3 - \frac{D}{2}\right), \\ \frac{x_3^2}{a^2} + \frac{y_3^2}{a^2 - (D/2)} &= 1, \\ \frac{x_3 - (D/2)}{\cos\left(-\beta_r^{n_3}\right)\cos\left(-\alpha_r^{n_3}\right)} &= \frac{y_3}{\cos\left(-\beta_r^{n_3}\right)\sin\left(-\alpha_r^{n_3}\right)} = \frac{z_3}{\sin\left(-\beta_r^{n_3}\right)}. \end{aligned} \tag{3}$$

The z coordinate of S_4 is a fixed value, which is equal to the vertical distance between the top surface of the ellipsoid and the xoy plane. The x and y coordinates can be expressed as

$$\begin{aligned} x_4 &= \frac{z_4}{\sin\left(-\beta_r^{n_4}\right)\cos\left(-\alpha_r^{n_4}\right)\cos\left(-\beta_r^{n_4}\right)} + \frac{D}{2}, \\ y_4 &= \frac{z_4}{\sin\left(-\beta_r^{n_4}\right)\sin\left(-\alpha_r^{n_4}\right)\cos\left(-\beta_r^{n_4}\right)}. \end{aligned} \tag{4}$$

The path of the model considers three components, LoS, SB, and DB components. In particular, according to the principle of near and far, not all DB paths are considered. The specific paths are shown in Table 1. Based on the above model description and scatterer calculation, a series of 6G channel parameters such as 6G channel impulse response, power delay spectrum, delay spread, 6G channel transfer function, and frequency correlation function can be obtained.

For the reference model, we assume that the number of scatterers is infinite, that is, $N_1, N_2, N_3, N_4 \longrightarrow \infty$. The impulse response of the 6G channel can be expressed as the cumulative sum of three components:

$$h(\tau) = h_{Los}(\tau) + h_{SB}(\tau) + h_{DB}(\tau). \tag{5}$$

The 6G channel impulse response of the LoS component can be expressed as

$$h_{Los}(\tau) = \sqrt{\frac{K}{K+1}} e^{-j2\pi f_c d_{\mathrm{LoS}}/c} \delta\left(\frac{\tau - d_{\mathrm{LoS}}}{c}\right), \tag{6}$$

where K is the Rice factor, which represents the ratio of LoS power to scattering power, fc = 300 GHz is the carrier frequency, $d_{LoS} = D$ is the distance of the LoS path, and c is the speed of light.

The 6G channel impulse response of the SB component can be expressed as

$$h_{SB}(\tau) = \sqrt{\frac{\eta_{SB}}{K+1}}\ \frac{1}{L}\sum_{l=1}^{K}\lim_{N_l \longrightarrow \infty}\frac{1}{\sqrt{N_l}}e^{j\varphi_{hj}-j2\pi f_c d_{nj}/c}\delta\left(\frac{\tau - d_{n_l}}{c}\right), \tag{7}$$

where η_{SB} is the ratio of the power of the SB path to the power of the NLoS path, $L = 4$ is the type of SB scatterer, and Nl is the number of scatterers 1S. d is the distance of the path Tx-Sl-Rx, which can be calculated by Euclidean formula:

$$d_{n_l} = \sqrt{\left(x_l + \frac{D}{2}\right)^2 + y_l^2 + z_l^2} + \sqrt{\left(x_l - \frac{D}{2}\right)^2 + y_l^2 + z_l^2}. \tag{8}$$

The 6G channel impulse response of the DB component can be expressed as

$$h_{SB}(\tau) = \sqrt{\frac{\eta_{DB}}{K+1}}\ \frac{1}{LM}\sum_{l=1}^{K}\sum_{m=1}^{M}\frac{1}{\sqrt{N_l N_m}} \times \sum_{n_1=1}^{N_l}\sum_{n_m=1}^{N_m} e^{j\varphi_{hj}-j2\pi f_c d_{nj}/c}\delta\left(\frac{\tau - d_{n_l n_m}}{c}\right), \tag{9}$$

where η_{DB} is the ratio of the power of the DB path to the power of the NLoS path, L is the type of the first hop scatterer, M is the type of the second hop scatterer, and $L = M = 4$. $d_{n_l n_m}$ is the distance of the path Tx-Sl-Sm-Rx, which can also be calculated as

$$d_{n_1 n_m} = \sqrt{\left(x_l + \frac{D}{2}\right)^2 + y_t^2 + z_t^2} + \sqrt{\left(x_m + \frac{D}{2}\right)^2 + y_m^2 + z_m^2} + \sqrt{(x_m - x_l)^2 + (y_m - y_l)^2 + (z_m - z_l)^2}. \tag{10}$$

Based on the reference model, a sine accumulation simulation model can be obtained. In the reference model, the number of scatterers is assumed to be infinite, while the simulation model discretizes the parameters to further simplify the reference model. The SB and DB components can be simplified as

$$h_{SB}(\tau) = \sqrt{\frac{\eta_{SB}}{K+1}}\ \frac{1}{\sqrt{L}}\sum_{l=1}^{L}\frac{1}{\sqrt{N_l}}e^{j\varphi_{hj}-j2\pi f_c d_{nj}/c}\delta\left(\frac{\tau - d_{n_l}}{c}\right),$$
$$h_{DB}(\tau) = \sqrt{\frac{\eta_{DB}}{K+1}}\ \frac{1}{\sqrt{LM}}\sum_{l=1}^{K}\sum_{m=1}^{M}\frac{1}{\sqrt{N_l N_m}}\sum_{n_1=1}^{N_l}\sum_{n_m=1}^{N_m} e^{j\varphi_{hj}-j2\pi f_c d_{nj}/c}\delta\left(\frac{\tau - d_{n_l n_m}}{c}\right). \tag{11}$$

This paper assumes that the phase is uniformly distributed at $[0, 2\pi)$. Azimuth angles of arrival (AAoA), elevation angles of arrival (EAoA), azimuth angles of departure (AAoD), and elevation angles of departure (EAoD) are subject to on Von-Miscs-Fisher (VMF) under different means and concentration levels, respectively, and are independent of each other. VMF distribution can be expressed as

$$f(x) = \frac{e^{k\cos(x - x_0)}}{2\pi I_0(k)}, \tag{12}$$

where x_0 is the mean, I_0 is the first kind of zero-order modified Bessel function, and k represents the concentration of the VMF distribution. The larger k is, the more concentrated the distribution of x is near x_o.

Based on the obtained 6G channel impulse response, the power delay profile (PDP) can be further calculated. The power delay spectrum describes the spread of the 6G channel in delay and is an important parameter to characterize the multi-path fading 6G channel. There are differences in the time for the signal to reach the receiving end through different paths, resulting in time spread. The power delay spectrum PDP can be expressed as the square of the 6G channel impulse response, that is:

$$\phi(\tau) = |h(\tau)|^2 = \left|h_{\mathrm{Los}}(\tau)\right|^2 + \left|h_{SB}(\tau)\right|^2 + \left|h_{DB}(\tau)\right|^2. \tag{13}$$

Due to the influence of multiple paths, the time of arrival spreads in the time domain. The average delay μ_τ and the root mean square delay spread (RMS) σ_τ can be used to describe the delay spread of the 6G channel. It can be calculated by the power delay spectrum PDP, expressed as

$$\mu_\tau = \frac{\sum_\tau \tau\phi(\tau)}{\sum_\tau \phi(\tau)},$$
$$\sigma_\tau = \sqrt{\frac{\sum_\tau (\tau - \mu_\tau)^2 \phi(\tau)}{\sum_\tau \phi(\tau)}}. \tag{14}$$

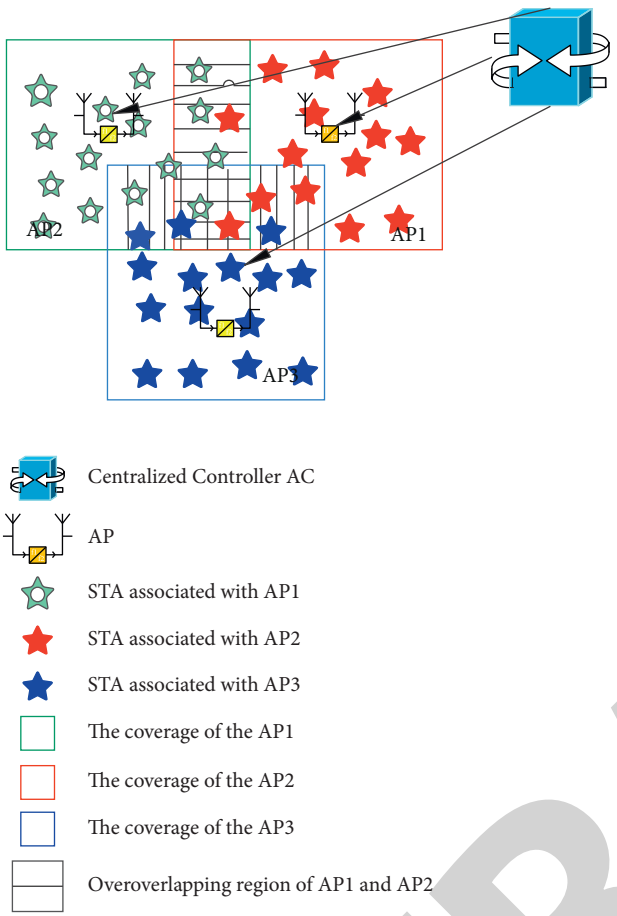

Figure 3: Schematic diagram of the network model.

The 6G channel transfer function (CTF) is obtained by the Fourier transform of the 6G channel impulse response, which describes the change of the signal in the frequency domain and can be expressed as

$$H(\tau) = H_{\mathrm{LoS}}(f) + H_{SB}(f) + H_{DB}(f). \tag{15}$$

Among them,

$$H_{LoS}(f) = \sqrt{\frac{K}{K+1}} e^{-j2\pi f_c d_{Los}/c - j2\pi f d_{nj}/c},$$

$$H_{SB}(\tau) = \sqrt{\frac{\eta_{SB}}{K+1}} \frac{1}{\sqrt{L}} \sum_{l=1}^{K} \lim_{N_l \longrightarrow \infty} \frac{1}{\sqrt{N_l}} e^{-j2\pi f_c d_{Los}/c - j2\pi f d_{nj}/c},$$

$$H_{DB}(f) = \sqrt{\frac{\eta_{DB}}{K+1}} \frac{1}{\sqrt{LM}} \sum_{l=1}^{L} \sum_{m=1}^{M} \frac{1}{\sqrt{N_l N_m}} \times \sum_{n_1=1}^{N_l} \sum_{n_m=1}^{N_m} e^{j\varphi_{n_j n_m} - j2\pi f_c d_{n_j n_m}/c - j2\pi f d_{n_j n_m}/c}. \tag{16}$$

The normalized frequency correlation function (FCF) is defined as

$$R(\Delta f) = \frac{E[H(f)H^*(f+\Delta f)]}{\sqrt{\mathrm{Var}[H(f)]\mathrm{Var}H^*[H^*(f+\Delta f)]}}. \tag{17}$$

The frequency correlation function describes the correlation degree of the signal at any two frequencies. $H_{SB}(f)$ and $H_{DB}(f)$ are mutually independent random processes, so the frequency correlation function can be further derived:

$$R(\Delta f) = R_{\mathrm{LoS}}(\Delta f) + R_{SB}(\Delta f) + R_{DB}(\Delta f). \tag{18}$$

Specifically,

$$R_{\mathrm{LoS}}(\Delta f) = \frac{K}{K+1} e^{(j2\pi\Delta f d_{LoS}/c)},$$

$$R_{SB}(\Delta f) = \frac{\eta_{SB}}{K+1} \frac{1}{\sqrt{L}} \sum_{l=1}^{L} E\left[e^{j2\pi\Delta f d_{NJ}/c}\right]$$

$$= \frac{\eta_{SB}}{K+1} \frac{1}{\sqrt{L}} \sum_{l=1}^{L} \int_{-\pi}^{\pi} \int_{(\pi/2)}^{(\pi/2)} e^{(j2\pi\Delta f \mathrm{d}_{\mathrm{LoS}}/2)} f(a_r^{n_l}) a(\beta_r^{n_l}) \mathrm{d}a_r^{n_l} \mathrm{d}\beta_r^{n_l}, \tag{19}$$

$$R_{DB}(\Delta f) = \frac{\eta_{DB}}{K+1} \frac{1}{\sqrt{LM}} \sum_{l=1}^{L} \sum_{m=1}^{M} E\left[e^{j2\pi\Delta f d_{LoS}/c}\right]$$

$$= \frac{\eta_{DB}}{K+1} \frac{1}{\sqrt{LM}} \sum_{l=1}^{L} \sum_{m=1}^{M} \int_{-\pi}^{\pi} \int_{(\pi/2)}^{(\pi/2)} \int_{-\pi}^{\pi} \int_{(\pi/2)}^{(\pi/2)} e j2\pi\Delta f \mathrm{d}_{NJ}/c.$$

Among them, $f(\alpha_t^{n_l}), f(\beta_t^{n_l}), f(\alpha_r^{n_m}), f(\beta_r^{n_m})$ is the probability density distribution function of the horizontal departure angle, the pitch departure angle, the horizontal arrival angle, and the pitch arrival angle, respectively.

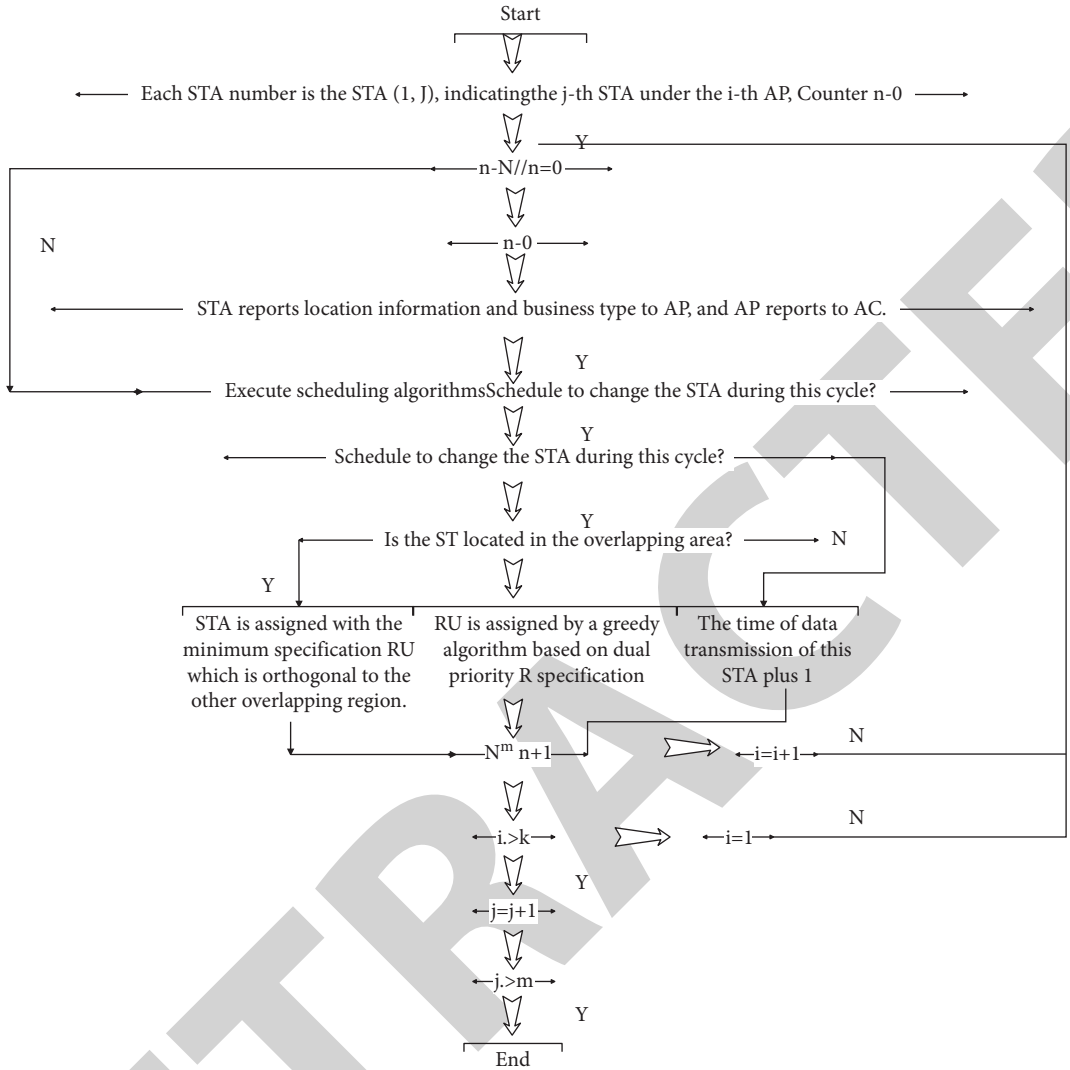

Figure 4: The overall flowchart of the algorithm.

4. Smart System Resource Coordination Based on 6G Technology

There are L service types in the network, and each service type has different delay restrictions. Each STA has only one service type, and different STAs may have different service types. When multiple APs send data to STAs in the overlap area at the same time, each STA in the overlap area will receive signals from multiple APs at the same time and suffer severe interference. The network model is shown in Figure 3.

This paper designs an algorithm for maximizing throughput scheduling and resource allocation based on user delay to meet the user's access delay limit and reduce interference in overlapping areas and improve the system throughput of the entire network. The general idea of the algorithm is as follows: based on AC unified scheduling between APs and STAs, time-sharing scheduling of different types of services is used to ensure the transmission delay of different types of services. In the resource allocation stage, the goal is to maximize system throughput. Based on the idea of greedy algorithm and traversal, under the premise of ensuring that all scheduled STAs are allocated RUs, users with better channel quality are first allocated RUs of higher specifications. If STAs located in the OBSS area and belonging to different BSSs are scheduled at the same time, it is necessary to allocate orthogonal RUs for them as much as possible to reduce the co-channel interference of users in the overlapping area and improve the overall system throughput. Taking UL transmission as an example, the overall flow of the algorithm is shown in Figure 4.

As shown in Figure 5, when the coverage areas of multiple APs have overlapping areas, if STAs located in the OBSS area are scheduled at the same time and the same or overlapping RUs are used to transmit data, serious interference will occur. In order to solve the above-mentioned problems, the users in the overlapping area are given priority to allocate mutually orthogonal minimum specification RUs, which can not only avoid the interference of the same

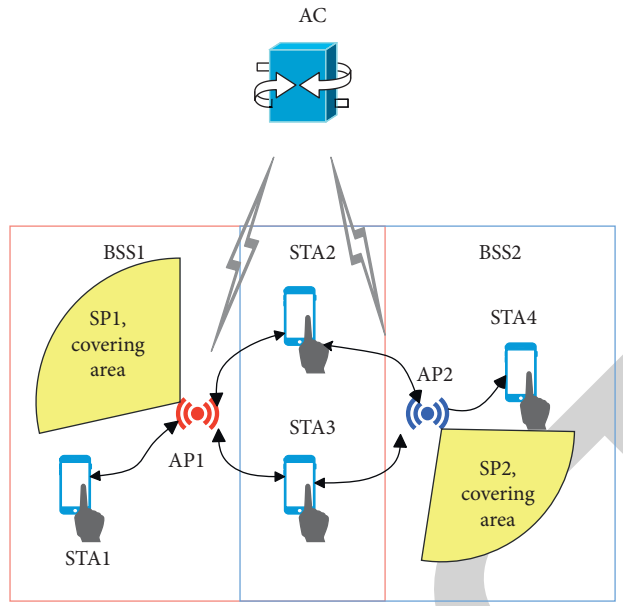

Figure 5: Schematic diagram of user interference.

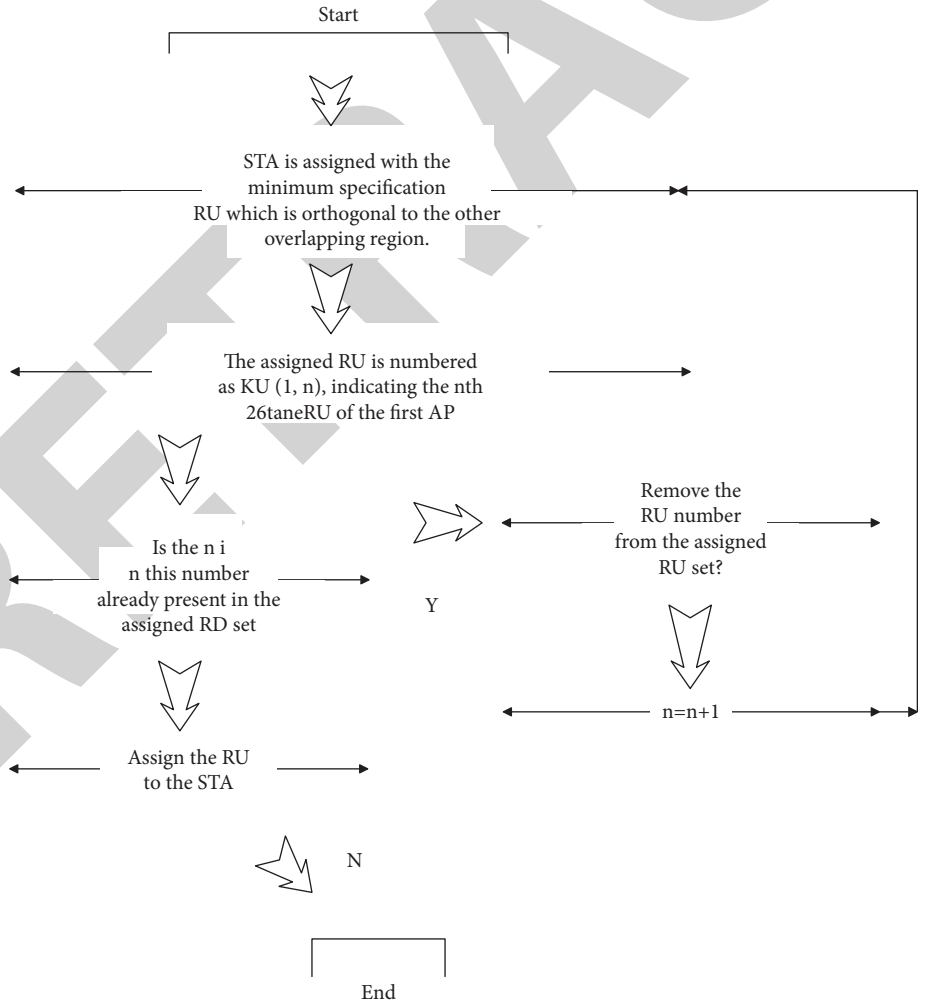

Figure 6: Flowchart of allocating mutually orthogonal RUs.

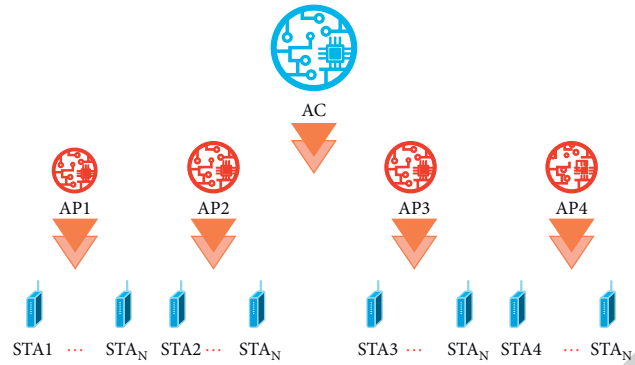

Figure 7: Topology diagram of long-distance Wi-Fi network scenario.

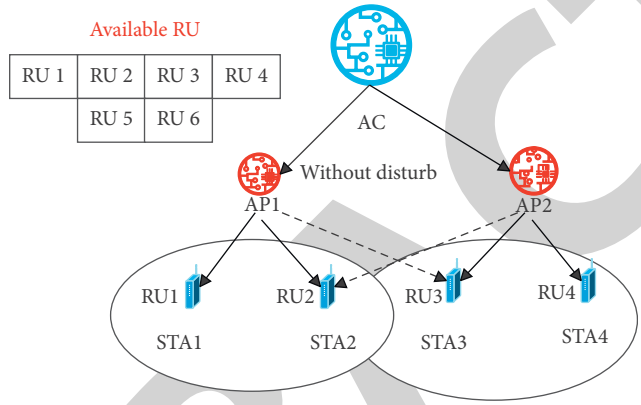

Figure 8: Anti-interference method based on AC scheduling.

Table 2: Resource coordination effects of smart systems based on 6G technology.

No.	Resource coordination	No.	Resource coordination
1	84.93	18	84.12
2	88.03	19	93.87
3	93.28	20	87.96
4	86.29	21	92.04
5	88.09	22	92.80
6	85.07	23	86.84
7	93.66	24	87.15
8	85.52	25	86.57
9	93.73	26	88.73
10	90.98	27	89.92
11	86.67	28	90.81
12	89.93	29	93.79
13	84.39	30	92.18
14	90.58	31	84.06
15	87.90	32	85.48
16	90.74	33	90.26
17	86.23	34	90.35

frequency in the overlapping area but also meet the transmission delay requirements of the users in the overlapping area. The process of assigning RU to a single overlapping area user is shown in Figure 6.

The STA in the overlap area and the STA at the edge of the AP signal coverage cannot perform data transmission or the transmission rate is low. In response to the above situation, this paper designs a centralized control-based transmission mechanism based on IEEE 802.11ax, including a greedy algorithm for resource allocation based on priority sorting and a resource adjustment mechanism for overlapping areas. Two different priority ranking schemes are

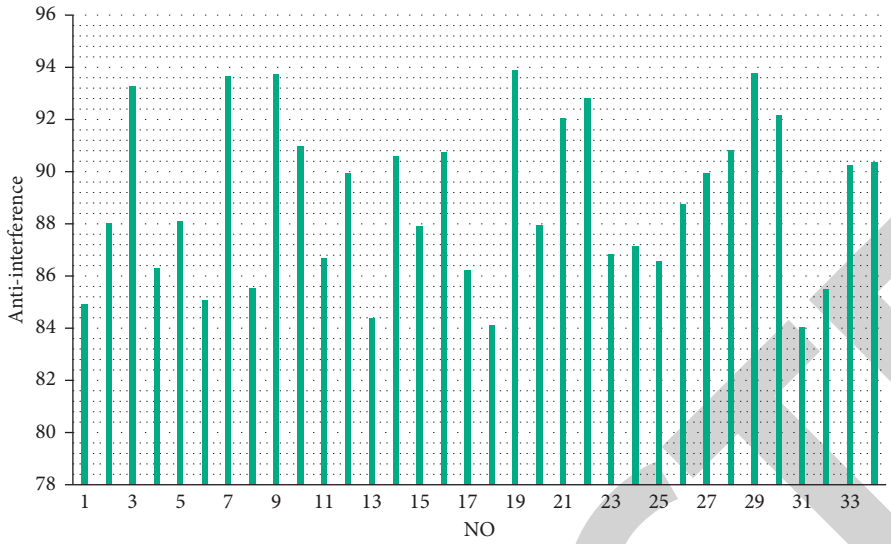

Figure 9: Statistical diagram of the evaluation of resource coordination of smart systems.

Table 3: Evaluation of anti-jamming performance of smart system resource coordination algorithm based on 6G technology.

No.	Anti-interference	No.	Anti-interference
1	74.40	18	80.85
2	67.24	19	80.36
3	79.99	20	71.48
4	73.98	21	61.03
5	68.51	22	80.43
6	78.04	23	80.65
7	63.22	24	62.86
8	76.59	25	73.09
9	69.32	26	76.52
10	79.57	27	73.28
11	73.94	28	65.65
12	61.19	29	65.18
13	80.86	30	69.76
14	73.06	31	70.37
15	76.03	32	74.45
16	77.69	33	66.10
17	76.30	34	73.74

proposed, which can flexibly choose between maximizing system throughput and user fairness according to the business, as shown in Figure 7.

In dense networking scenarios, concurrent APs with the same frequency that are close together will cause huge interference to the other party. However, if AP deployment is reduced for this reason or the distance between the two is greatly increased, the number of terminals that the system can serve will also be greatly reduced, and the user experience cannot be improved. If the AC is used for centralized scheduling at this time, as shown in Figure 8, the AC performs centralized management and control through the collected interference information. Moreover, through flexible scheduling and resource division strategies, the interference intensity between adjacent co-frequency BSSs can be reduced, and the system throughput can be improved. In addition, AC allocates RU resources with orthogonal time/frequency dimensions to users of each BSS, so that multiple BSSs on the same frequency can achieve concurrent communication, and the number of terminal devices that the system can serve can be greatly increased.

On the basis of the above research, the intelligent system resource coordination algorithm based on 6G technology in this paper is studied. First, the resource coordination effect of the system in this paper is verified, and the results shown in Table 2 and Figure 9 are obtained.

From the above research, it can be seen that the smart system resource coordination algorithm based on 6G technology proposed in this paper can play an important role in smart system resource coordination, and then the anti-interference effect of the algorithm is evaluated, and the results shown in Table 3 and Figure 10 are obtained.

Through the above experimental research, it can be seen that the smart system resource coordination algorithm based on 6G technology proposed in this paper can effectively improve the anti-interference ability of the smart system and

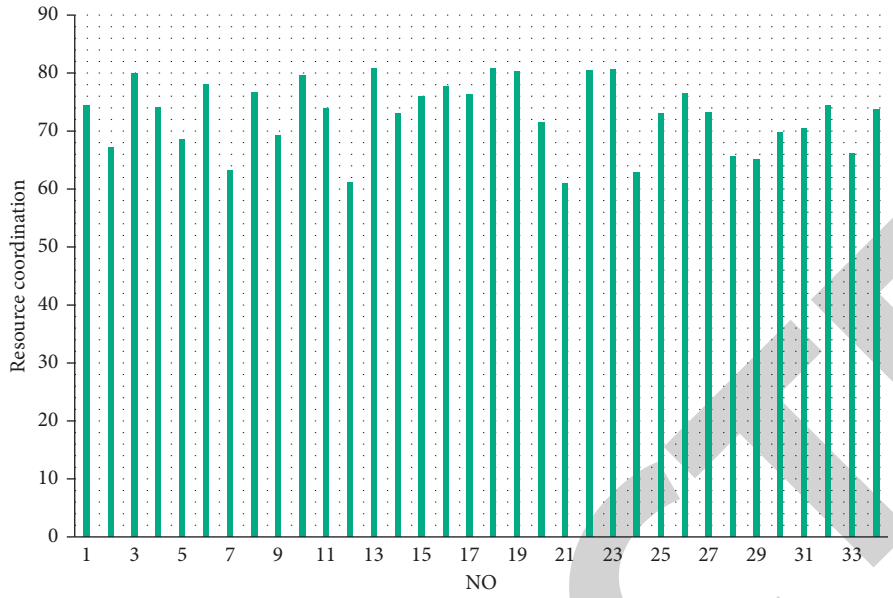

Figure 10: Statistical diagram of the evaluation of the anti-interference effect of the system.

has an important supporting role in its internal resource coordination.

5. Conclusion

With the explosive growth of the number of smart terminal devices, people's demand for the capacity of WLAN networks is gradually increasing. In order to provide people with a better network access experience and increase the overall network capacity and coverage, more and more APs are deployed in densely populated places such as our campuses, residences, offices, and squares. This type of multi-AP deployment model will become mainstream in the future. With the gradual increase in the number of APs, the distance between adjacent APs is getting closer and closer. If the number is too large, the interference will be extremely serious, and the system throughput will be greatly reduced. Based on the 6G technology, this paper studies the smart system resource coordination algorithm, proposes an improved method, and verifies its effectiveness, so as to provide a theoretical reference for the further popularization and development of the follow-up 6G technology.

Data Availability

The labeled dataset used to support the findings of this study is available from the corresponding author upon request.

Conflicts of Interest

The author declares that there are no conflicts of interest.

References

[1] J. E. Siegel, S. Kumar, and S. E. Sarma, "The future internet of things: secure, efficient, and model-based," *IEEE Internet of Things Journal*, vol. 5, no. 4, pp. 2386–2398, 2018.

[2] M. A. Abd-Elmagid, N. Pappas, and H. S. Dhillon, "On the role of age of information in the internet of things," *IEEE Communications Magazine*, vol. 57, no. 12, pp. 72–77, 2019.

[3] A. Sheth, U. Jaimini, and H. Y. Yip, "How will the internet of things enable augmented personalized health?[J]," *IEEE Intelligent Systems*, vol. 33, no. 1, pp. 89–97, 2018.

[4] G. J. Joyia, R. M. Liaqat, A. Farooq, M. Rao, and S. Rehman, "Internet of Medical Things (IOMT): applications, benefits and future challenges in healthcare domain," *Journal of Communication*, vol. 12, no. 4, pp. 240–247, 2017.

[5] N. Kshetri, "The evolution of the internet of things industry and market in China: an interplay of institutions, demands and supply," *Telecommunications Policy*, vol. 41, no. 1, pp. 49–67, 2017.

[6] S. Siboni, V. Sachidananda, Y. Meidan et al., "Security t for internet-of-things devices," *IEEE Transactions on Reliability*, vol. 68, no. 1, pp. 23–44, 2019.

[7] Y. Yang, M. Zhong, H. Yao, F. Yu, X. Fu, and O. Postolache, "Internet of things for smart ports: t," *IEEE Instrumentation and Measurement Magazine*, vol. 21, no. 1, pp. 34–43, 2018.

[8] Z. Li, Y. Liu, A. Liu, S. Wang, and H. Liu, "Minimizing c time and energy consumption in green internet of things," *IEEE Transactions on Emerging Topics in Computing*, vol. 8, no. 3, pp. 797–813, 2020.

[9] P. P. Ray, "A survey on Internet of Things architectures," *Journal of King Saud University-Computer and Information Sciences*, vol. 30, no. 3, pp. 291–319, 2018.

[10] M. Mayer and A. J. Baeumner, "A megatrend challenging analytical chemistry: biosensor and c concepts ready for the internet of things," *Chemical Reviews*, vol. 119, no. 13, pp. 7996–8027, 2019.

[11] M. Saez, F. P. Maturana, K. Barton, and D. M. Tilbury, "Real-time manufacturing machine and system performance monitoring using internet of things," *IEEE Transactions on Automation Science and Engineering*, vol. 15, no. 4, pp. 1735–1748, 2018.

[12] V. Jagadeeswari, V. Subramaniyaswamy, R. Logesh, and V. Vijayakumar, "A study on medical Internet of Things and Big Data in personalized healthcare system," *Health Information Science and Systems*, vol. 6, no. 1, pp. 14–20, 2018.

[13] S. Smys, A. Basar, and H. Wang, "Hybrid intrusion detection system for internet of Things (IoT)," *Journal of ISMAC*, vol. 2, no. 04, pp. 190–199, 2020.

[14] I. Butun, P. Österberg, and H. Song, "Security of the internet of things: vulnerabilities, attacks, and countermeasures," *IEEE Communications Surveys & Tutorials*, vol. 22, no. 1, pp. 616–644, 2020.

[15] T. Qiu, N. Chen, K. Li, M. Atiquzzaman, and W. Zhao, "How can heterogeneous internet of things build our future: a survey," *IEEE Communications Surveys & Tutorials*, vol. 20, no. 3, pp. 2011–2027, 2018.

[16] A. Heiskanen, "The technology of trust: h," *Construction Research and Innovation*, vol. 8, no. 2, pp. 66–70, 2017.

[17] M. Wolf and D. Serpanos, "Safety and security in cyber-physical systems and internet-of-things systems," *Proceedings of the IEEE*, vol. 106, no. 1, pp. 9–20, 2018.

[18] S. Dotsenko, O. Illiashenko, S. Kamenskyi, and V. Kharchenko, "Integrated security management system for enterprises in industry 4.0," *Information and security: an international journal*, vol. 43, no. 3, pp. 294–304, 2019.

[19] N. Y. Kim, S. Rathore, J. H. Ryu, and J H. Park, "A survey on cyber physical system security for IoT: issues, challenges, threats, solutions," *Journal of Information Processing Systems*, vol. 14, no. 6, pp. 1361–1384, 2018.

[20] S. U. Hani and A. T. Alam, "Software development for information system - achieving optimum quality with security," *International Journal of Information System Modeling and Design*, vol. 8, no. 4, pp. 1–20, 2017.